Advances in Nano Research, *Vol. 18, No. 2 (2025) 133-142*
https://doi.org/10.12989/anr.2025.18.2.133

Vibration of nonuniform mass sensor nanobeams with considering size effects at nano-scale

Mostafa Nazemizadeh*[1], Behrooz Shahriari[1a], Waseem Dalla[1b] and Moein Taheri[2c]

[1]*Faculty of Mechanics, Malek Ashtar University of Technology, Iran*
[2]*Department of Mechanical Engineering, Faculty of Engineering, Arak University, Arak, Iran*

(*Received May 28, 2020, Revised December 6, 2024, Accepted February 11, 2025*)

Abstract. This study focuses on the precise modeling and frequency analysis of a mass-sensing nanobeam, utilizing the nonlocal elasticity theory while accounting for longitudinal discontinuities. It is posited that the beam can absorb both lumped and distributed masses, leading to the establishment of an innovative general formulation for the system. The energy Eqs. for the beam are formulated with the consideration of the longitudinal discontinuities and the arbitrary absorbed masses, leading to the derivation of vibration Eqs. and boundary conditions for the non-uniform nanobeam through Hamilton's principle. An analytical solution is employed, assuming the number of shape functions matches the longitudinal discontinuities present. By defining the compatibility and boundary conditions, we derive and resolve the frequency Eq. pertinent to the discontinuous nanobeam. The investigation explores the effects of various parameters, including the sensed mass and size effects, on the frequency characteristics of the nanobeam across different vibrational modes. The results highlight the importance of accurately modeling the discontinuous nanobeam. Notably, relocating the sensed mass towards the free end of the cantilever beam enhances the sensing performance, whereas size effects generally reduce it. Furthermore, the findings reveal that the mass-sensing capabilities of the nanobeam are more pronounced at higher vibrational modes, suggesting a preference for deploying the nanobeam mass sensor in these modes.

Keywords: absorbed masses; distributed and lumped; general formulation; mass sensor; nanobeam; nonuniform; size effects

1. Introduction

Recent advancements in engineering technologies have facilitated the development of small-scale systems ats micron and submicron levels. Over the past few decades, nano-scale technologies have led to the creation and implementation of sophisticated micro/nanosystems, including atomic force microscopes (AFMs), nanoactuators, and nano-sensors (Syahmazgi 2014, Bakhtiari-Nejad 2016, Letti 2017, Ouakad 2020). Nano-scale beams are notable for their small dimensions, ease of manufacturing, and high-frequency performance, making them key vibrational components in nanosystems. Additionally, an important characteristic of nanobeams is their displacement and deformation due to elasticity. This property, combined with the challenges associated with fabricating small-scale joints, has resulted in their widespread application in nano-technology systems. While micro/nanobeams can operate in either static or dynamic modes, they are predominantly utilized in resonant vibrational modes for most applications. Consequently, the resonant vibration characteristics—such as frequency response and sensitivity—of these small beams are critical for enhancing their performance and efficiency.

Jiang *et al*. (2011) conducted a dynamic modeling and vibration analysis of a nanobeam resonator, proposing a numerical solution to ascertain the vibration characteristics of nanobeams under nano-scale deformations. Carvalho *et al*. (2013) investigated a cantilever nanobeam subjected to a concentrated axial load and lateral harmonic excitation. They formulated nonlinear differential Eqs. governing the beam's motion and derived a set of discretized Eqs. of motion using the Galerkin method. Although classical continuum theory is employed to model nanobeams, it often fails to accurately represent continuous systems at submicron scales.

Conversely, experiments and molecular simulations conducted at the micro and nano scales have revealed the effects of size-dependent mechanical behavior on micro/nano systems (Yueguang 2003, Chen 2006). The mechanical properties and behavior of micro/nanobeams are inherently linked to their dimensions at small scales; classical elasticity theory lacks the capacity to adequately interpret these size effects. Moreover, conducting experimental tests at the micro and nano scales is both challenging and costly. Consequently, over the last few decades, size-dependent elasticity theories have been developed for the dynamic analysis of small-scale systems, garnering significant interest among researchers in the field of nanoscience. Akgöz and Civalek (2013) examined the size-dependent free vibrational characteristics of non-uniform composite microbeams based on modified couple stress theory. Jalali *et al*. (2018) explored the size-dependent vibrations of a functionally graded micro- resonator using the same

*Corresponding author, Assistant Professor,
E-mail: nazemi@mut-es.ac.ir
[a] Associate Professor, E-mail: Shahriari@mut-es.ac.ir
[b] Ph.D. Student, E-mail: waseemdalla@mut-es.ac.ir
[c] Associate Professor, E-mail: m-taheri@araku.ac.ir

ISSN: 2287-237X (Print), 2287-2388 (Online)

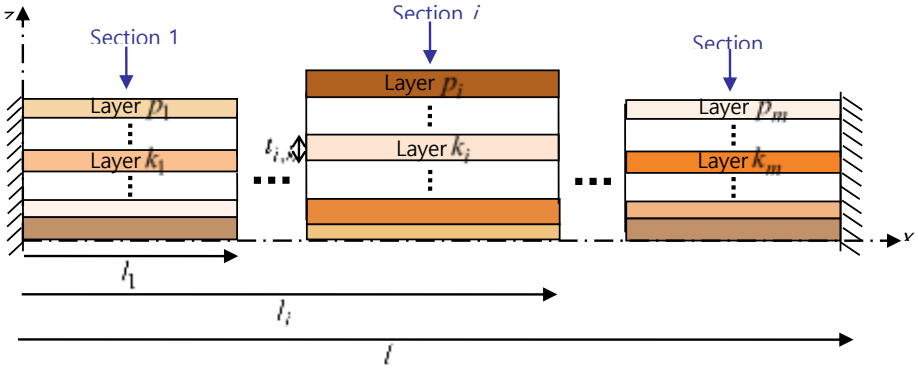

Fig. 1 A nonunifom nanobeam

modified couple stress theory, employing the Rayleigh-Ritz method to obtain the size-dependent natural frequencies of the beam under various boundary conditions. Assadi and Nazemizadeh (2021) investigate size-dependent vibrations of stepped nanobeams taken into account surface elasticity theory. They concluded that surface effects and appropriate steps selection have noticeable impact on natural frequencies of non-uniform nanobeams.

In addition, the nonlocal size-dependent elasticity theory has emerged over the past two decades, attracting considerable attention from nanotechnology researchers. This theory was first introduced by Eringen in 1977, and its initial application in modeling nanoscale systems was conducted by Pedison in 2003. Pedison modeled a nonlocal nanobeam, demonstrating its critical role in micro/nano-technology applications. Demir and Civalek (2013) analyzed the size effects on torsional and axial responses of microbeams using a nonlocal continuum rod model. Nazemizadeh and Bakhtiari-Nejad (2015) investigated the free vibrations of micro/nanobeams with piezoelectric layers, focusing on the size effects that influence the vibrational behavior of nonlocal beams and highlighting the significant impact of the nonlocal parameter on the dynamic characteristics of the nanobeam.

Aydogdu *et al*. (2018) addressed the vibrations of functionally graded nanobeams based on nonlocal elasticity theory, utilizing the Ritz method with algebraic polynomials to calculate natural frequencies across varying boundary conditions and material properties. Nazemizadeh *et al*. (2020) studied the nonlinear vibrations of piezoelectric laminated nanobeams, applying the Galerkin separation method and the multiple-scale perturbation method to derive an analytical expression for the nonlinear natural frequencies of the system. They also explored the size effects on the nonlinear vibrations of piezoelectric laminated nanobeams at higher modes based on nonlocal piezoelectric theory. Assadi *et al*. (2022) studied size-dependent vibration of single-crystalline rectangular nanoplates with cubic anisotropy considering surface stress and nonlocal elasticity effects. The results indicate that size scale parameters have different vibration effects at different material orientations and boundary conditions. Nalbant *et al*. (2023) contributed to the free vibration analysis of stepped nanobeams using nonlocal elasticity theory, basing their beam analysis on Bernoulli-Euler theory, with nano-scale analysis grounded in Eringen's nonlocal elasticity theory. Moreover, Hang and Pen (2024) investigated the in-plane bending vibrations of L-shaped cantilever nanobeams carrying a tip nanoparticle via nonlocal elasticity, comparing the exact resonance frequencies of the system to those of a corresponding macro-scale L-shaped cantilever, revealing that the nonlocal parameter reduces the resonance frequencies.

In this article, we present a vibration analysis of mass-sensor nanobeams with lumped and distributed sensed mass, considering both longitudinal discontinuities and nonlocal elasticity theory. The non-uniform and discontinuous model of nanobeams is inspired by the observation that most micro/nanobeams are designed and fabricated with narrower end sections. Therefore, we consider a discontinuous nanobeam model that can sense arbitrary masses at a specified longitudinal point, applicable for mass sensor purposes. To derive the governing vibrational Eqs., we develop the beam energy relations while accounting for the discontinuity, ultimately obtaining the vibrational Eqs. and boundary conditions of the nonlocal nanobeam in accordance with Hamilton's principle. For the number of longitudinal discontinuities, we ensure that the same number of mode shape responses aligns along the nanobeam using an analytical solution. The frequency Eq. for the discontinuous mass-sensor nanobeam is derived as an algebraic relationship by applying compatibility conditions and nonlocal boundary conditions. We calculate the natural frequencies across various modes of the nanobeam by solving the frequency response, investigating the influence of several parameters, such as the length of discontinuity, sensed mass, and the nonlocal parameter on the frequency behavior of the nanobeam. Furthermore, we simulate the effects of sensed mass and size on the shape functions of the nanobeam, focusing particularly on these effects at higher modes to assess the application and efficiency of the mass sensor in those vibrational modes.

2. Governing Equations of the system

In this section, we derive the governing vibrational Eq. of a general nonuniform nanobeam based on nonlocal continuum theory. The nanobeam exhibits arbitrary

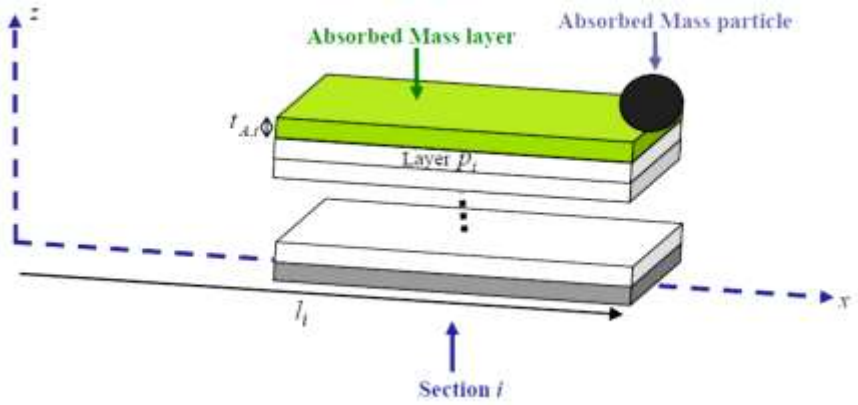

Fig. 2 A schematic of the *i*th longitudinal section of the mass sensor

longitudinal discontinuities and is capable of sensing both layered and lumped masses. Fig. 1 illustrates the structure of the discontinuous nanobeam:

As previously mentioned, the mass sensor is capable of absorbing both lumped and layered masses. A schematic representation of the *i*th longitudinal section of the mass sensor is shown in Fig. 2.

Unlike classical continuum mechanics, nonlocal elasticity theory posits that the stress components at a given point depend not only on the strain components at that same point but also on the strain states of all other points within the medium. Consequently, for homogeneous and isotropic elastic solids, the nonlocal elasticity theory is formulated using the following Eqs. (Eringen 1977):

$$\sigma_{kl,l}^{nl} + \rho\left(f_k - \frac{\partial^2 u_k}{\partial t^2}\right) = 0 \tag{1}$$

$$\sigma_{kl}^{nl}(\vec{r}) = \int_V \alpha(|\vec{r} - \vec{r}'|, \chi)\, \sigma_{kl}^{l}(\vec{r}')dV(\vec{r}') \tag{2}$$

where σ_{kl}^{nl} denotes the nonlocal stress tensor, ρstates the mass density of the body, $\vec{r}$ is a reference point, f_k is given as the body force density, $\vec{u}$ denotes the displacement vector at the reference point $\vec{r}$ in the body, $\sigma_{kl}^{l}(\vec{r}')$ shows the classical stress tensor at any point $\vec{r}'$ in the body, V indicates the body volume, $|\vec{r} - \vec{r}'|$ is the distance in Euclidean form and χ is defined as a material constant. The nonlocal kernel $\alpha|x - x'|$ is given as the effect of the strain at the point $\vec{r}'$ on the stress at the point $\vec{r}$ in the elastic body. Thus, by presenting an appropriate nonlocal kernel, the nonlocal Eq. given by Eq. (2) is summerized to the differential Eq.:

$$\Re\sigma_{kl}^{nl} = \sigma_{kl}^{l} \tag{3}$$

where the differential operator is presumed as $\Re = 1 - \tau^2\nabla^2$, ∇^2 is the Laplacian operator and τ is the nonlocal scale coefficient that includes the size-dependent nano scale factor.

To derive the governing Eqs. of the micro/nano beam, an energy approach can be utilized. This requires the calculation of both the kinetic and elastic strain energies of the structure. The kinetic energy T of the structure is the summation of the kinetic energy of each section T_i and can be expressed as follows:

$$T = \sum_{i=1}^{m} T_i = \frac{1}{2}\sum_{i=1}^{m} \iiint_{V_i} \rho\dot{\vec{u}}^2\, dV_i \tag{4}$$

where $\vec{u}$ is the displacement vector at each point and $\rho$is the mass density of the point. Furthermore, the displacement vector is defined as $\vec{u} = \left[\bar{u}(x,t) - (z - \bar{z})\frac{\partial \bar{w}(x,t)}{\partial x} \quad 0 \quad \bar{w}(x,t)\right]^T$ in which $\bar{u}(x,t)$ and $\bar{w}(x,t)$ are the axial and transverse deflections in the centerline of the beam and $\bar{z}$ represents the neutral axis of the beam. So, the kinetic energy of *ith* section is expressed as:

$$\begin{aligned} T_i &= \frac{1}{2}\int_{l_{i-1}}^{l_i} \left\{ \iint_{A_i} \rho \left[\left(\frac{\partial \bar{w}_i(x,t)}{\partial t}\right)^2 \right] dA_i \right\} dx \\ &= \frac{1}{2}\int_{l_{i-1}}^{l_i} \left\{ (\rho A)_{eq,i} \left[\left(\frac{\partial \bar{w}_i(x,t)}{\partial t}\right)^2 \right] \right\} dx \end{aligned} \tag{5}$$

where $(\rho A)_{eq,i}$ is the equivalent mass inertia of the section and is equal:

$$(\rho A)_{eq,i} = \left(\sum_{k=1}^{p_i} \rho_{k,i} b_{k,i} h_{k,i} + \rho_{A,i} b_{A,i} h_{A,i} \right) \left(H_{l_{i-1}} - H_{l_i}\right) \tag{6}$$

where $\rho_{k,i}$, $b_{k,i}$ and $t_{k,i}$ represent the mass density, width and thickness of the *kth* layer of *ith* section of the beam, respectively. Moreover, $\rho_{A,i}$, $b_{A,i}$ and $t_{A,i}$ represent the mass density, width and thickness of the absorbed mass on the *ith* section of the beam. Also, $H_{l_i} = H(x - l_i)$ represents the Heavyside function. Furthermore, the elastic strain energy of the structure U is combination of the strain energy of each section of the beam, U_i as:

$$U = \sum_{i=1}^{m} U_i = \frac{1}{2}\sum_{i=1}^{m} \iiint_{V_i} \sigma_{xx}^{nl}\varepsilon_{xx} dV_i, \tag{7}$$

where σ_{xx}^{nl} is the nonlocal axial stress in the beam and the non-zero strain component ε_{xx} is equal to:

$$\varepsilon_{xx} = -(z-\bar{z})\frac{\partial^2 \bar{w}(x,t)}{\partial x^2} \tag{8}$$

The strains can be determined by differentiating the displacement Eq. provided earlier:

$$\bar{z}_i = \frac{1}{\sum_{k=1}^{p_i} E_{k,i} b_{k,i} h_{k,i} + E_{A,i} b_{A,i} h_{A,i}} \begin{bmatrix} \sum_{k=1}^{p_i} E_{k,i} b_{k,i}\, h_{k,i} \left(\sum_{j=1}^{k-1} h_{j,i} + \frac{1}{2} h_{k,i} \right) \\ + E_{A,i} b_{A,i} h_{A,i} \left(\sum_{j=1}^{p_i} h_{j,i} + \frac{1}{2} h_{A,i} \right) \end{bmatrix} \tag{9}$$

Now, by substituting Eq. (8) into (7), there will be:

$$\begin{aligned} U = \sum_{i=1}^{m} U_i &= \frac{1}{2}\sum_{i=1}^{m} \left\{ \int_{l_{i-1}}^{l_i} \iint_{A_i} \sigma_{xx,i}^{nl} \left[-(z - \bar{z}_i) \left(\frac{\partial^2 \bar{w}_i(x,t)}{\partial x^2} \right) \right] dA_i dx \right\} \\ &= \frac{1}{2}\sum_{i=1}^{m} \left\{ \int_{l_{i-1}}^{l_i} \left[-M_{xx,i}^{nl} \left(\frac{\partial^2 \bar{w}_i(x,t)}{\partial x^2} \right)^2 \right] dx \right\} \end{aligned} \tag{10}$$

where $M_{xx,i}^{nl}$ is the effective nonlocal moment in the *ith* section and is given as:

$$\begin{aligned} M_{xx,i}^{nl} &= \iint_{A_i} \sigma_{xx,i}^{nl} (z - \bar{z}_i) dA_i \\ &= \sum_{k=1}^{p_i} \int \sigma_{xx,i}^{nl} b_{i,k} (z - \bar{z}_i) dz \end{aligned} \tag{11}$$

Moreover, the work done by the non-conservative force $\pi_{n.c.}$ is defined as

$$\pi_{n.c.} = \frac{1}{2}\sum_{i=1}^{m} \left\{ \int_{l_i-1}^{l_i} \left[(q_{e,i} - q_{d,i}) \bar{w}_i(x,t) \right] dx \right\} \tag{12}$$

where $q_{e,i}$ and $q_{d,i}$ are the transverse distributed external force and the distributed transverse damping force. Furthermore, the Hamilton's principle states as:

$$\int_0^t (\delta T - \delta U + \delta \pi_{n.c.})\, dt = 0 \tag{13}$$

Now, by replacing Eqs. (5), (10), and (12) into (13), integrating by parts, and setting the coefficients of the $\delta \bar{w}_i(x,t)$ to zero; the resulting relation of vibration for the *i*th section of the beam is obtained as:

$$(\rho A)_{eq,i} \frac{\partial^2 \bar{w}_i(x,t)}{\partial t^2} = \frac{\partial^2 M_{xx,i}^{nl}}{\partial x^2} + q_{e,i} \tag{14}$$

Also, the boundary conditions are:

$$\left(\frac{\partial M_{xx,1}^{nl}}{\partial x} \right) \delta[\bar{w}_1(x,t)] \Big|_{x=0} = 0 \tag{15}$$

$$M_{xx,1}^{nl} \delta \left[\frac{\partial \bar{w}_1(x,t)}{\partial t} \right] \Big|_{x=0} = 0 \tag{16}$$

$$\bar{w}_i(l_i,t) = \bar{w}_{i+1}(l_i,t) \tag{17}$$

$$\frac{\partial \bar{w}_i(l_i,t)}{\partial x} = \frac{\partial \bar{w}_{i+1}(l_i,t)}{\partial x} \tag{18}$$

$$M_{xx,i}^{nl}(l_i,t) = M_{xx,i+1}^{nl}(l_i,t) \tag{19}$$

$$\frac{\partial M_{xx,i}^{nl}(l_i,t)}{\partial x} = \frac{\partial M_{xx,i+1}^{nl}(l_i,t)}{\partial x} \tag{20}$$

$$\left(\frac{\partial M_{xx,m}^{nl}}{\partial x} \right) \delta[\bar{w}_m(x,t)] \Big|_{x=l} = 0 \tag{21}$$

$$M_{xx,m}^{nl} \delta \left[\frac{\partial \bar{w}_m(x,t)}{\partial t} \right] \Big|_{x=l} = 0 \tag{22}$$

Moreover, for the nonlocal mass sensor beam, the one-dimensional form of the governing Eq. (3) is:

$$\sigma_{xx}^{nl} - \tau^2 \frac{\partial^2 \sigma_{xx}^{nl}}{\partial x^2} = E \varepsilon_{xx} \tag{23}$$

where E is Young's modulus of the beam. Also, for the section *i* of the beam, Eq. (23) is rewritten as:

$$\sigma_{xx,i}^{nl} - \tau^2 \frac{\partial^2 \sigma_{xx,i}^{nl}}{\partial x^2} = E_i \left[-(z - \bar{z}_i) \frac{\partial^2 \bar{w}_i(x,t)}{\partial x^2} \right] \tag{24}$$

Now, by integrating Eq. (24) with respect to relations (8) and (11), the following relation is obtained:

$$M_{xx,i}^{nl} - \tau^2 \frac{\partial^2 M_{xx,i}^{nl}}{\partial x^2} = -(EI)_{eq,i} \frac{\partial^2 \bar{w}_i(x,t)}{\partial x^2} \tag{25}$$

where the equivalent rigidity is stated as:

$$(EI)_{eq,i} = \begin{Bmatrix} \sum_{k=1}^{p_i} E_{k,i} b_{k,i} h_{k,i} \left\{ \frac{1}{12} h_{k,i}^2 + \left[\bar{z}_i - \left(\sum_{j=1}^{k-1} h_{j,i} + \frac{1}{2} h_{k,i} \right) \right]^2 \right\} \\ + E_{A,i} b_{A,i} h_{A,i} \left\{ \frac{1}{12} h_{A,i}^2 + \left[\bar{z}_i - \left(\sum_{j=1}^{p_i} h_{j,i} + \frac{1}{2} h_{A,i} \right) \right]^2 \right\} \end{Bmatrix} \left(H_{l_{i-1}} - H_{l_i} \right) \tag{26}$$

Also, submitting Eq. (11) into (25) results in:

$$\begin{aligned} M_{xx,i}^{nl} = \tau^2 &\left[(\rho A)_{eq,i} \frac{\partial^2 \bar{w}_i(x,t)}{\partial t^2} - q_{e,i} \right] \\ &- (EI)_{eq,i} \frac{\partial^2 \bar{w}_i(x,t)}{\partial x^2} \end{aligned} \tag{27}$$

Now, by replacing Eq. (27) into (11), the governing relation of nanobeam vibration is achieved as:

$$\begin{aligned} &\left(1 - \tau^2 \frac{\partial^2}{\partial x^2} \right) (\rho A)_{eq,i} \frac{\partial^2 \bar{w}_i(x,t)}{\partial t^2} \\ &= \frac{\partial^2}{\partial x^2} \left[-(EI)_{eq,i} \frac{\partial^2 \bar{w}_i(x,t)}{\partial x^2} \right] + (1 - \tau^2 \frac{\partial^2}{\partial x^2}) q_{e,i} \end{aligned} \tag{28}$$

Therefore, for any longitudinal section of the nanosensor, the transverse vibration Eqs. and boundary conditions of the nonlocal mass sensing nanobeam are concluded as:

$$\sum_{i=1}^{m}\left\{(1-\tau^2\frac{\partial^2}{\partial x^2})\left[(\rho A)_{eq,i}\frac{\partial^2\bar{w}_i(x,t)}{\partial t^2}\right]+\frac{\partial^2}{\partial x^2}\left[(EI)_{eq,i}\frac{\partial^2\bar{w}_i(x,t)}{\partial x^2}\right]-(1-\tau^2\frac{\partial^2}{\partial x^2})q_{e,i}\right\}=0 \tag{29}$$

$$\frac{\partial}{\partial x}\left[-(EI)_{eq,1}\frac{\partial^2\bar{w}_1(x,t)}{\partial x^2}+\tau^2(\rho A)_{eq,1}\frac{\partial^2\bar{w}_1(x,t)}{\partial t^2}\right]\delta[\bar{w}_1(x,t)]\Big|_{x=0}=0 \tag{30}$$

$$\left[-(EI)_{eq,1}\frac{\partial^2\bar{w}_1(x,t)}{\partial x^2}+\tau^2(\rho A)_{eq,1}\frac{\partial^2\bar{w}_1(x,t)}{\partial t^2}\right]\delta\left[\frac{\partial\bar{w}_1(x,t)}{\partial t}\right]\Big|_{x=0}=0 \tag{31}$$

$$\bar{w}_i(x,t)|_{x=l_i}=\bar{w}_{i+1}(l_i,t)|_{x=l_i} \tag{32}$$

$$\frac{\partial\bar{w}_i(x,t)}{\partial x}\Big|_{x=l_i}=\frac{\partial\bar{w}_{i+1}(x,t)}{\partial x}\Big|_{x=l_i} \tag{33}$$

$$\left[-(EI)_{eq,i}\frac{\partial^2\bar{w}_i(x,t)}{\partial x^2}+\tau^2(\rho A)_{eq,i}\frac{\partial^2\bar{w}_i(x,t)}{\partial t^2}\right]\Big|_{x=l_i}=\left[-(EI)_{eq,i+1}\frac{\partial^2\bar{w}_{i+1}(x,t)}{\partial x^2}+\tau^2(\rho A)_{eq,i+1}\frac{\partial^2\bar{w}_{i+1}(x,t)}{\partial t^2}\right]\Big|_{x=l_i} \tag{34}$$

$$\begin{Bmatrix}\frac{\partial}{\partial x}\left[-(EI)_{eff,i}\frac{\partial^2\bar{w}_i(x,t)}{\partial x^2}+\mu^2l^2(\rho A)_{eff,i}\frac{\partial^2\bar{w}_i(x,t)}{\partial t^2}\right]+M_{A,i}\frac{\partial^2\bar{w}_i(x,t)}{\partial t^2}\Big|_{x=l_i}\\ -\frac{\partial}{\partial x}\left[-(EI)_{eff,i+1}\frac{\partial^2\bar{w}_{i+1}(x,t)}{\partial x^2}+\mu^2l^2(\rho A)_{eff,i+1}\frac{\partial^2\bar{w}_{i+1}(x,t)}{\partial t^2}\right]\Big|_{x=l_i}\end{Bmatrix}=0 \tag{35}$$

$$\frac{\partial}{\partial x}\left[-(EI)_{eq,m}\frac{\partial^2\bar{w}_m(x,t)}{\partial x^2}+\tau^2(\rho A)_{eq,m}\frac{\partial^2\bar{w}_m(x,t)}{\partial t^2}\right]\delta[\bar{w}_m(x,t)]\Big|_{x=l}=0 \tag{36}$$

$$\left[-(EI)_{eff,m}\frac{\partial^2\bar{w}_m(x,t)}{\partial x^2}+\mu^2l^2(\rho A)_{eff,m}\frac{\partial^2\bar{w}_m(x,t)}{\partial t^2}+M_{A,m}\frac{\partial^2\bar{w}_m(x,t)}{\partial t^2}\right]\delta\left[\frac{\partial\bar{w}_m(x,t)}{\partial t}\right]\Big|_{x=l}=0 \tag{37}$$

3. Solution of the problem

In the preceding section, we derived the governing Eqs. and boundary conditions for the nanobeam. To analytically solve the vibration Eq. of the nanobeam with the sensed mass, the governing Eq. for the *i*-th section of the nonlocal nanobeam, in the absence of external forces, is expressed as follows:

$$(\rho A)_{eq,i}\frac{\partial^2\bar{w}_i(x,t)}{\partial t^2}-\tau^2\frac{\partial^2}{\partial x^2}\left[(\rho A)_{eq,i}\frac{\partial^2\bar{w}_i(x,t)}{\partial t^2}\right]+\frac{\partial^2}{\partial x^2}\left[(EI)_{eq,i}\frac{\partial^2\bar{w}_i(x,t)}{\partial x^2}\right]=0 \tag{38}$$

Now, a length scale is defined as $\bar{x}=x/l$ and Eq. (61) is rewritten as:

$$(\rho A)_{eq,i}\frac{\partial^2\bar{w}_i(x,t)}{\partial t^2}-\bar{\mu}\frac{\partial^2}{\partial\bar{x}^2}\left[(\rho A)_{eq,i}\frac{\partial^2\bar{w}_i(x,t)}{\partial t^2}\right]+\frac{1}{l^4}\frac{\partial^2}{\partial\bar{x}^2}\left[(EI)_{eq,i}\frac{\partial^2\bar{w}_i(x,t)}{\partial\bar{x}^2}\right]=0 \tag{39}$$

where $\bar{\mu}=\mu^2$ and $\mu=\frac{\tau}{l}$exhibits the nonlocal effects on the beam. Moreover, the response of free vibration of the ith section is considered as $\bar{w}_i(\bar{x},t)=\phi_i(\bar{x})e^{j\omega_nt}$ where $j=\sqrt{-1}$. By substituting the solution into the governing Eq. along with the boundary and compatibility conditions, we can derive the solution. By defining $\bar{l}_i=l_i/l$ and the non-dimensional parameter $\chi_{n,i}$ as a function of the nth natural frequency of the beam, the natural frequency can be expressed as:

$$\omega_n=\left(\frac{(EI)_{eq,i}}{(\rho A)_{eq,i}}\right)^{\frac{1}{2}}\left(\frac{\chi_{n,i}}{l}\right)^2 \tag{40}$$

$$\begin{aligned}\phi_i(\bar{x})=&\,k_{1,i}\,sin(\delta_i\bar{x})+k_{2,i}\,cos(\delta_i\bar{x})\\&+k_{3,i}\,sinh(\eta_i\bar{x})+k_{4,i}\,cosh(\eta_i\bar{x})\end{aligned} \tag{41}$$

where the following relations are considered:

$$\delta_i=\frac{\bar{\mu}\,\chi_{n,i}^4}{2}+\left[\chi_{n,i}^4+\left(\frac{\bar{\mu}\,\chi_{n,i}^4}{2}\right)^2\right]^{\frac{1}{2}} \tag{42}$$

$$\eta_i = -\frac{\bar{\mu}\,\chi_{n,i}^4}{2} + \left[\chi_{n,i}^4 + \left(\frac{\bar{\mu}\,\chi_{n,i}^4}{2}\right)^2\right]^{\frac{1}{2}} \tag{43}$$

Now, submitting the solution given by Eq. (41) into boundary conditions (30)-(37) gives the following algebraic Eqs. in matrix from that are linear with respect to the coefficient vector $\vec{K}$:

$$\begin{matrix} \underbrace{\phi_1 \quad \phi_2 \quad \cdots \quad \phi_i \quad \phi_{i+1} \quad \cdots \quad \phi_{m-1} \quad \phi_m} \\ \left.\begin{matrix} \bar{x}=0 \\ \bar{x}=\bar{l}_1 \\ \vdots \\ \bar{x}=\bar{l}_i \\ \vdots \\ \bar{x}=\bar{l}_{m-1} \\ \bar{x}=1 \end{matrix}\right\} \end{matrix} \begin{bmatrix} [\hat{C}_0]_{2\times4} & [0]_{2\times4} & \cdots & \cdots & \cdots & \cdots & \cdots & [0]_{2\times4} \\ [\hat{A}_1]_{4\times4} & [\hat{B}_1]_{4\times4} & [0]_{4\times4} & \cdots & \cdots & \cdots & \cdots & [0]_{4\times4} \\ \vdots & \vdots & \vdots & \vdots & \vdots & \vdots & \vdots & \vdots \\ [0]_{4\times4} & \cdots & \cdots & [\hat{A}_i]_{4\times4} & [\hat{B}_i]_{4\times4} & [0]_{4\times4} & \cdots & [0]_{4\times4} \\ \vdots & \vdots & \vdots & \vdots & \vdots & \vdots & \vdots & \vdots \\ [0]_{4\times4} & \cdots & \cdots & \cdots & \cdots & [0]_{4\times4} & [\hat{A}_{m-1}]_{4\times4} & [\hat{B}_{m-1}]_{4\times4} \\ [0]_{2\times4} & \cdots & \cdots & \cdots & \cdots & \cdots & [0]_{2\times4} & [\hat{C}_m]_{2\times4} \end{bmatrix} \vec{K} = \vec{0} \tag{44}$$

where $\vec{K} = [k_{1,1}\, k_{2,1}\, k_{3,1}\, k_{4,1} \ldots k_{1,m}\, k_{2,m}\, k_{3,m}\, k_{4,m}]$, the $[0]$ is a zero matrix and the following relations are considered as

$$\hat{A}_i = \begin{bmatrix} sin(\delta_i\bar{l}_i) & cos(\delta_i\bar{l}_i) & sinh(\eta_i\bar{l}_i) & cosh(\eta_i\bar{l}_i) \\ \delta_i\, cos(\delta_i\bar{l}_i) & -\delta_i\, sin(\delta_i\bar{l}_i) & \eta_i\, cos(\eta_i\bar{l}_i) & \eta_i\, sinh(\eta_i\bar{l}_i) \\ (EI)_{eq,i}(\bar{\mu}\chi_i^4 - \delta_i^2)\, sin(\delta_i\bar{l}_i) & (EI)_{eq,i}(\bar{\mu}\chi_i^4 - \delta_i^2)\, cos(\delta_i\bar{l}_i) & (EI)_{eq,i}(\bar{\mu}\chi_i^4 + \eta_i^2)\, sinh(\eta_i\bar{l}_i) & (EI)_{eq,i}(\bar{\mu}\chi_i^4 + \eta_i^2)\, cosh(\eta_i\bar{l}_i) \\ \hat{a}_{4,1} & \hat{a}_{4,2} & \hat{a}_{4,3} & \hat{a}_{4,4} \end{bmatrix} \tag{45}$$

$$\hat{B}_i = \begin{bmatrix} -sin(\delta_{i+1}\bar{l}_i) & -cos(\delta_{i+1}\bar{l}_i) & -sinh(\eta_{i+1}\bar{l}_i) & -cosh(\eta_{i+1}\bar{l}_i) \\ -\delta_{i+1}\, cos(\delta_{i+1}\bar{l}_i) & \delta_{i+1}\, sin(\delta_{i+1}\bar{l}_i) & -\eta_{i+1}\, cos(\eta_{i+1}\bar{l}_i) & -\eta_{i+1}\, sinh(\eta_{i+1}\bar{l}_i) \\ -(EI)_{eq,i+1}\left(\begin{matrix}\bar{\mu}\chi_{i+1}^4 \\ -\delta_{i+1}^2\end{matrix}\right) sin(\delta_{i+1}\bar{l}_i) & -(EI)_{eq,i+1}\left(\begin{matrix}\bar{\mu}\chi_{i+1}^4 \\ -\delta_{i+1}^2\end{matrix}\right) cos(\delta_{i+1}\bar{l}_i) & -(EI)_{eq,i+1}\left(\begin{matrix}\bar{\mu}\chi_{i+1}^4 \\ +\eta_{i+1}^2\end{matrix}\right) sinh(\eta_{i+1}\bar{l}_i) & -(EI)_{eq,i+1}\left(\begin{matrix}\bar{\mu}\chi_{i+1}^4 \\ +\eta_{i+1}^2\end{matrix}\right) cosh(\eta_{i+1}\bar{l}_i) \\ \hat{b}_{4,1} & \hat{b}_{4,2} & \hat{b}_{4,3} & \hat{b}_{4,4} \end{bmatrix} \tag{46}$$

where some coefficients of matrix can be written as:

$$\begin{aligned} \hat{a}_{4,1} &= (EI)_{eq,i}\left[\delta_i\left(\bar{\mu}\chi_{n,i}^4 - \delta_i^2\right) cos\left(\delta_i\bar{l}_i\right) + \bar{m}_{A,i}\chi_{n,i}^4\, sin\left(\delta_i\bar{l}_i\right)\right] \\ \hat{a}_{4,2} &= -(EI)_{eq,i}\left[\delta_i\left(\bar{\mu}\chi_{n,i}^4 - \delta_i^2\right) sin\left(\delta_i\bar{l}_i\right) + \bar{m}_{A,i}\chi_{n,i}^4\, cos\left(\delta_i\bar{l}_i\right)\right] \\ \hat{a}_{4,3} &= (EI)_{eq,i}\left[\eta_i\left(\bar{\mu}\chi_{n,i}^4 + \eta_i^2\right) cosh\left(\eta_i\bar{l}_i\right) + \bar{m}_{A,i}\chi_{n,i}^4\, sinh\left(\eta_i\bar{l}_i\right)\right] \\ \hat{a}_{4,4} &= (EI)_{eq,i}\left[\eta_i\left(\bar{\mu}\chi_{n,i}^4 + \eta_i^2\right) sinh\left(\eta_i\bar{l}_i\right) + \bar{m}_{A,i}\chi_{n,i}^4\, cosh\left(\eta_i\bar{l}_i\right)\right] \end{aligned} \tag{47}$$

$$\begin{aligned} \hat{b}_{4,1} &= -(EI)_{eq,i+1}\left[\delta_{i+1}\left(\bar{\mu}\chi_{n,i+1}^4 - \delta_{i+1}^2\right) cos\left(\delta_{i+1}\bar{l}_i\right) + \bar{m}_{A,i+1}\chi_{n,i+1}^4\, sin\left(\delta_{i+1}\bar{l}_i\right)\right] \\ \hat{b}_{4,2} &= (EI)_{eq,i+1}\left[\delta_{i+1}\left(\bar{\mu}\chi_{n,i+1}^4 - \delta_{i+1}^2\right) sin\left(\delta_{i+1}\bar{l}_i\right) + \bar{m}_{A,i+1}\chi_{n,i+1}^4\, cos\left(\delta_{i+1}\bar{l}_i\right)\right] \\ \hat{b}_{4,3} &= -(EI)_{eq,i+1}\left[\eta_{i+1}\left(\bar{\mu}\chi_{n,i+1}^4 + \eta_{i+1}^2\right) cosh\left(\eta_{i+1}\bar{l}_i\right) + \bar{m}_{A,i+1}\chi_{n,i+1}^4\, sinh\left(\eta_{i+1}\bar{l}_i\right)\right] \\ \hat{b}_{4,4} &= -(EI)_{eq,i+1}\left[\eta_{i+1}\left(\bar{\mu}\chi_{n,i+1}^4 + \eta_{i+1}^2\right) sinh\left(\eta_{i+1}\bar{l}_i\right) + \bar{m}_{A,i+1}\chi_{n,i+1}^4\, cosh\left(\eta_{i+1}\bar{l}_i\right)\right] \end{aligned} \tag{48}$$

Also the matrices $[\hat{C}_0]$ and $[\hat{C}_m]$ are related to the boundary conditions at $x = 0$ and $x = l$, respectively. According to clamped-free boundary conditions, the following relations can be stated:

$$[C_0] = \begin{bmatrix} 0 & 1 & 0 & 1 \\ \delta_1 & 0 & \eta_1 & 0 \end{bmatrix} \tag{49}$$

$$[C_m] = \begin{bmatrix} sin(\delta_m)\,(\bar{\mu}\chi_m^4 - \delta_m^2) & cos(\delta_m)\,(\bar{\mu}\chi_m^4 - \delta_m^2) & sinh(\eta_m)\,(\bar{\mu}\chi_m^4 + \eta_m^2) & cosh(\eta_m)\,(\bar{\mu}\chi_m^4 + \eta_m^2) \\ C_{2,1} & C_{2,2} & C_{2,3} & C_{2,4} \end{bmatrix} \tag{50}$$

where the coefficients of the matrix are:

$$\begin{aligned} C_{2,1} &= \delta_m\, cos(\delta_m)\,(\bar{\mu}\chi_m^4 - \delta_m^2) + \bar{m}_{A,m}\chi_{n,m}^4\, sin\,\delta_m \\ C_{2,2} &= -\delta_m\, sin(\delta_m)\,(\bar{\mu}\chi_m^4 - \delta_m^2) + \bar{m}_{A,m}\chi_{n,m}^4\, cos\,\delta_m \\ C_{2,3} &= \eta_m\, cosh(\eta_m)\,(\bar{\mu}\chi_m^4 + \eta_m^2) + \bar{m}_{A,m}\chi_{n,m}^4\, sinh\,\eta_m \\ C_{2,4} &= \eta_m\, sinh(\eta_m)\,(\bar{\mu}\chi_m^4 + \eta_m^2) + \bar{m}_{A,m}\chi_{n,m}^4\, cosh\,\eta_m \end{aligned} \tag{51}$$

where the non-dimensional lumped mass is defined as $\bar{m}_{A,i} = \frac{M_{A,i}}{(\rho A)_{eq,i}\,l}$. Therefore, a non-zero solution of Eq. (77) is found only when the determinant of the characteristic matrix is set to zero. This condition defines the characteristic Eq. of the vibrating nonlocal mass sensor, where the solution provides the nonlocal frequency of the beam. An alternative approach, which can be quite interesting, involves calculating the non-dimensional parameter χ_i (or $\chi_{n,i}$) instead of the nth natural frequency ω_n. To do this, considering Eq. (73), one can express each $\chi_{n,j}$ as functions of a specific parameter of the ith section of the beam $\chi_{n,i}$:

$$\chi_{n,j} = \left[\frac{(\rho A)_{eq,j}(EI)_{eq,i}}{(\rho A)_{eq,i}(EI)_{eq,j}}\right]^{\frac{1}{4}} \chi_{n,i} \quad (52)$$

Next, by replacing Eqs. (45)-(52) into (44) and letting the determinant of the characteristics Eq. zero, we arrive at the characteristic Eq. of the mass sensing beam as a nonlinear function of $\chi_{n,i}$. Solving this Eq. yields parameter $\chi_{n,i}$ and subsequently the nth natural frequency ω_n.

4. Simulation results

In this section, we will simulate the frequency analysis of the mass sensor nanobeam at higher modes. The simulations are done for a nanobeam with two longitudinal sections. The physical and geometrical characteristics of the nanobeam are summarized in Table 1:

First, to verify the presented solution, the first dimensionless natural frequency of the nanobeam is compared with the values presented by Pedieson (2003). The case study focuses on a uniform nanobeam without any sensed mass

Furthermore, in the first simulation, we investigate the effect of accurately modeling the nanobeam on its frequency behavior. For this purpose, the nonlocal discontinuous nanobeam, as the precise model, is compared with several inaccurate models: the local discontinuous beam, the nonlocal uniform beam, and the local uniform beam. It is assumed that the sensed mass is located at the free end of the nanobeam, and the natural frequency of the beam is calculated accordingly.

In Table 3, the first natural frequency and its relative error for each model, compared to the exact model (nonlocal discontinuous beam), are presented in MHz, assuming the nonlocal parameter is zero.

Table 3 illustrates that the effect of discontinuity is significant in the accurate modeling of the nanobeam. The relative error introduced by applying a continuous model is non-negligible when compared to the discontinuous model, highlighting the importance of precise modeling in this work.

For another simulation, we consider a cantilever nanobeam that has absorbed a particle at its free end. The natural frequency shift is defined as $\Delta f = f_0 - f_1$ where f_0 the natural frequency of the beam without the sensed particle, and f_1 is the natural frequency of the beam with the sensed particle. Fig. 3 show the frequency shift of the nanobeam at 1st and 2nd modes of vibration:

As seen in Fig. 3, the frequency shift increases as the added mass increases. Additionally, both the nonlocal coefficient and the vibration mode influence the nonlocal effects on frequency shift, with greater values resulting in larger shifts. It is important to note that as the vibration mode increases, both the resonance frequency and the frequency shift also rise, suggesting that the application of beam sensing improves at higher vibration modes.

Table 1 characteristics of mass sensing nanobeam

Physical characteristics			Geometric Specification (nm)				
Material	Density (kg/m^3)	Young's modulus (Gpa)	l_1	l_2	$t_1 = t_2$	h_1	h_2
sio_2	2330	107	120	60	20	10	5

Table 2 Comparison of the first dimensionless natural frequency

R	μ	Current research	(Pedieson 2003)
0	0	1.8751	1.8751
	0.1	1.8792	1.8791
	0.2	18919	1.8917

Table 3 First natural frequency (MHz) of the nanobeam considering different models

	First Frequency			
	R=0		R=0.5	
	Value	Error (%)	Value	Error (%)
Nonlocal stepped beam	1.261	-	0.654	-
Classic stepped beam	1.249	0.95	0.651	0.458
Nonlocal stepped beam	1.357	7.6	0.776	18.65
Classic stepped beam	1.352	7.21	0.775	18.50

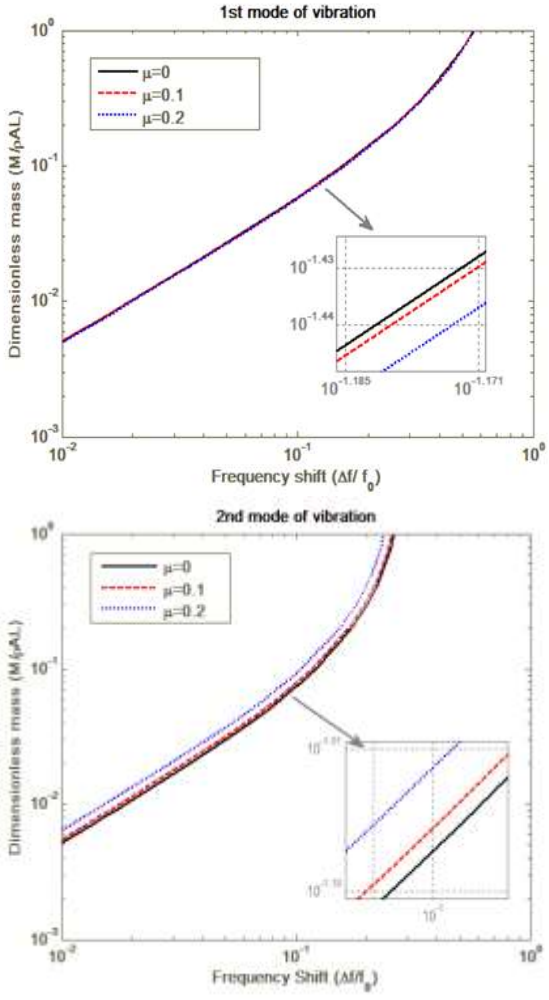

Fig. 3 Frequency shift of the mass sensor nanobeam

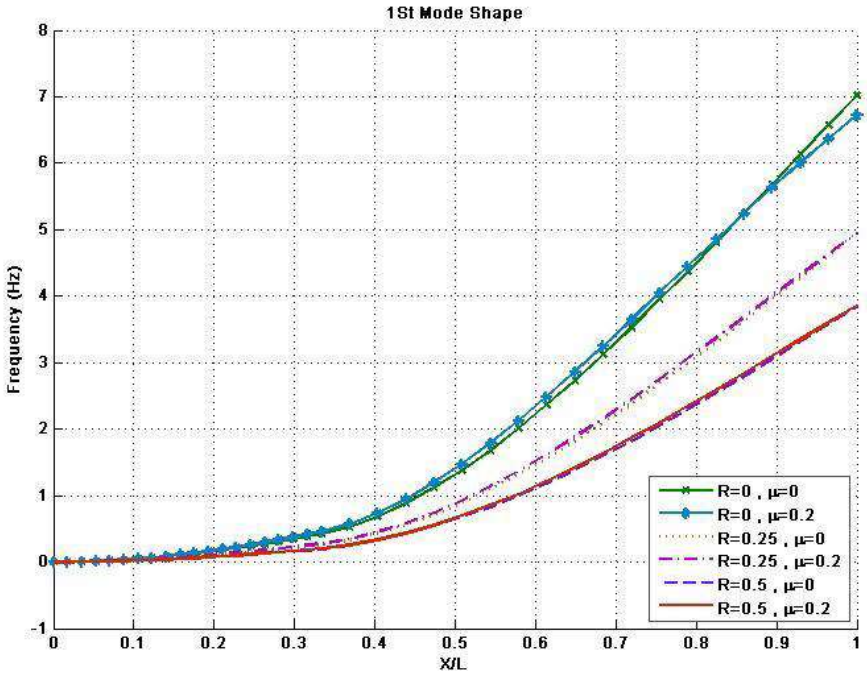

Fig. 4 First shape function of the nanobeam for different sensed mass

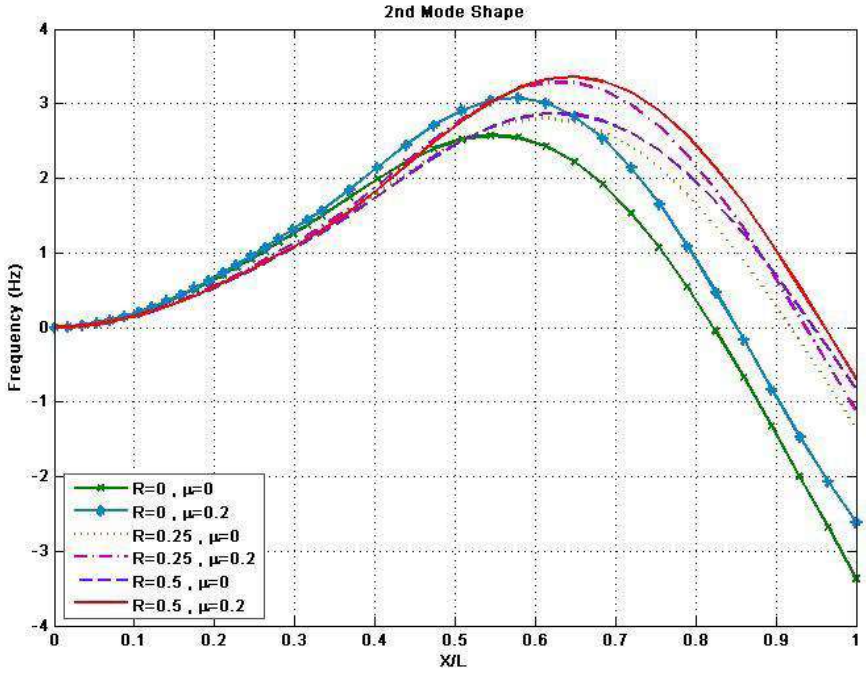

Fig. 5 Second shape function of the nanobeam for different sensed mass

In another study, we examine the effect of the nonlocal parameter on the mode shapes of the mass sensor nanobeam for different absorbed masses at its end. Fig. 4 shows the shape function for the first mode of the beam:

As observed in Fig. 4, increasing the nonlocal term and size effects results in a slight increase in the amplitude of the first mode of the nanobeam. However, these size effects diminish as the sensed mass increases. Conversely, the amplitude of the mode shape decreases with an increase in the absorbed mass. This reduction occurs because the increase in sensed mass raises the total inertia of the mass sensor nanobeam, leading to a decrease in the amplitude at the free end of the nanobeam.

Furthermore, the shape function of the second mode of the sensor nanobeam for different absorbed masses at the end of the beam is depicted in Fig. 5.

As shown in Fig. 5, increasing the nonlocal term in the second vibrational mode enhances the amplitude of the mode shape. This increase can be attributed to the nonlocal term reducing the stiffness of the nanobeam, thereby

Table 4 Effect of thickness $\bar{h}$ on the first and second natural frequencies (MHz)

μ	R	$\bar{h}$	ω_1	ω_1
0	0	0.3	0.2172	1.2310
		0.6	0.3346	1.6212
	0.25	0.3	0.1382	0.9942
		0.6	0.2241	1.3467
0.1	0	0.3	0.2195	1.1145
		0.6	0.3385	1.5183
	0.25	0.3	0.1390	0.9052
		0.6	0.2251	1.2681

increasing the vibrational amplitude. Similarly, the amplitude of the mode shape decreases with an increase in the absorbed mass. It is also noted that as the sensed mass increases, the influence of the nonlocal term on the mode shape of the nanobeam decreases.

In another simulation, as presented in Table 4, the frequency behavior of both classical and nonlocal nano-beams is investigated for different thickness ratios $\bar{h} = \frac{h_2}{h_1}$.

As illustrated in Table 4, increasing the thickness of the nanobeam results in a higher natural frequency. This is because increasing the thickness enhances both the mass and stiffness of the nanobeam simultaneously; however, the effect on stiffness is more pronounced than on structural mass. Additionally, as the thickness increases, the ratio of frequency reduction for the sensed mass nanobeam decreases.

5. Conclusions

In this paper, we have conducted precise modeling of the nanobeam, considering discontinuity based on size-dependent nonlocal elasticity theory. The vibrational Eqs. and boundary conditions for the mass sensor nanobeam were derived using Hamilton's principle. Subsequently, the frequency Eq. for the discontinuous nanobeam was formulated as an algebraic relation through an analytical solution, taking into account the sensed mass.

The study investigates the effects of various parameters, including the length of discontinuity, sensed mass, and nonlocal parameters, on the frequency behavior of the nanobeam. The results indicate that the effect of discontinuity is critical for accurate modeling of the nanobeam and must be considered; however, an increase in sensed mass leads to a reduction in the relative modeling error.

Furthermore, the influence of the nonlocal term and size effects is significant at higher vibrational modes and should be incorporated into nanobeam modeling. It is also observed that as the position of the sensed mass is adjusted toward the free end of the nanobeam, the natural frequency decreases while its sensing sensitivity increases. Additionally, increasing the thickness of the nanobeam enhances the stiffness of the structure and raises its natural frequency, but it concurrently reduces the sensitivity of the mass sensor nanobeam.

References

Akgöz, B. and Civalek, Ö. (2013), "Free vibration analysis of axially functionally graded tapered Bernoulli–Euler micro beams based on the modified couple stress theory", *Compos. Struct.*, **98**, 314-322. https://doi.org/ 10.5829/IJE.2021.34.03C.20

Assadi, A. and Nazemizadeh, M. (2021), "Size-dependent vibration analysis of stepped nanobeams based on surface elasticity theory", *Int. J. Eng.*, **34**(3), 744-749. https://doi.org/10.12989/anr.2018.6.3.257

Assadi, A., Najaf, H. and Nazemizadeh, M. (2022), "Size-dependent vibration of single-crystalline rectangular nanoplates with cubic anisotropy considering surface stress and nonlocal elasticity effects", *Thin Wall. Struct.*, **170**, 108518. https://doi.org/10.1016/j.tws.2021.108518

Aydogdu, M., Arda, M. and Filiz, S. (2018), "Vibration of axially functionally graded nano rods and beams with a variable nonlocal parameter", *Adv. Nano Res.*, **6**(3), 257. https://doi.org/10.12989/anr.2018.6.3.257

Bakhtiari-Nejad, F. and Nazemizadeh, M. (2016), "Size-dependent dynamic modeling and vibration analysis of MEMS/NEMS-based nanomechanical beam based on the nonlocal elasticity theory", *Acta Mechanica*, **227**(5), 1363-1379. https://doi.org/10.1007/s00707-015-1556-3.

Carvalho, E.C., Gonçalves, P.B., Rega, G. and Del Prado, Z.J. (2013), "Influence of axial loads on the nonplanar vibrations of cantilever beams", *Shock Vib.*, **20**(6), 1073-1092. https://doi.org/10.3233/SAV-130823

Chen, C.Q., Shi, Y., Zhang, Y.S., Zhu, J. and Yan, Y.J. (2006), "Size dependence of Young's modulus in ZnO nanowires", *Phys. Rev. Lett.*, **96**(7), 075505. https://doi.org/10.1103/PhysRevLett.96.075505

Demir, C. and Civalek, Ö. (2013), "Torsional and longitudinal frequency and wave response of microtubules based on the nonlocal continuum and nonlocal discrete models", *Appl. Math. Modell.*, **37**(22), 9355-9367. https://doi.org/10.1016/j.apm.2013.04.050

Eringen, A.C. (1977). "Screw dislocation in non-local elasticity", *J. Phys. D Appl. Phys.*, **10**(5), 671. https://doi.org 10.1088/0022-3727/10/5/009/meta

Feng, C., Jiang, L. and Lau, W.M. (2011), "Dynamic characteristics of a dielectric elastomer-based microbeam resonator with small vibration amplitude", *J. Micromech. Microeng.*, **21**(9), 095002. https://doi.org/10.1088/0960-1317/21/9/095002/meta.

Jalali, M.H., Zargar, O and Baghani, M. (2019), "Size-dependent vibration analysis of FG microbeams in thermal environment based on modified couple stress theory", *Iran. J. Sci. Technol. T. Mech. Eng.*, **43**(1), 761-771. https://doi.org/10.1007/s40997-018-0193-6

Jiang, L.Y. and Yan, Z. (2010), "Timoshenko beam model for static bending of nanowires with surface effects", *Physica E*, **42**(9), 2274-2279. https://doi.org/10.1016/j.physe.2010.05.007

Letti, C.J., Costa, K.A., Gross, M.A., Paterno, L.G., Pereira-da-Silva, M.A., Morais, P.C and Soler, M.A. (2017), "Synthesis, morphology and electrochemical applications of iron oxide based nanocomposites", *Adv. Nano Res.*, **5**(3), 215. https://doi.org/10.12989/anr.2017.5.3.215.

Nalbant, M.O., Bagdatli, S.M. and Tekin, A. (2023), "Free vibrations analysis of stepped nanobeams using nonlocal elasticity theory", *Scientia Iranica*, In press. https://doi.org/10.24200/SCI.2023.61602.7395

Nazemizadeh, M. and Bakhtiari-Nejad, F. (2015), "Size-dependent free vibration of nano/microbeams with piezo-layered actuators". *Micro Nano Lett.*, **10**(2), 93-98. https://doi.org/10.1049/mnl.2014.0317

Ouakad, H.M., Sedighi, H.M. and Al-Qahtani, H.M. (2020), "Forward and backward whirling of a spinning nanotube nano-rotor assuming gyroscopic effects", *Adv. Nano Res.*, **8**(3), 245. https://doi.org/10.12989/anr.2020.8.3.245.

Nazemizadeh, M., Bakhtiari-Nejad, F., Assadi, A. and Shahriari, B. (2020), "Size-dependent nonlinear dynamic modeling and vibration analysis of piezo-laminated nanomechanical resonators using perturbation method", *Arch. Appl. Mech.*, **90**, 1659-1672. https://doi.org/10.1007/s00419-020-01678-3

Nazemizadeh, M., Bakhtiari-Nejad, F., Assadi, A. and Shahriari, B. (2020), "Nonlinear vibration of piezoelectric laminated nano-beams at higher modes based on nonlocal piezoelectric theory", *Acta Mechanica*, **231**, 4259-4274. https://doi.org/10.1007/s00707-020-02736-1

Peddieson, J., Buchanan, G.R. and McNitt, R.P. (2003), "Application of nonlocal continuum models to nanotechnology", *Int. J. Eng. Sci.*, **41**(3-5), 305-312. https://doi.org/10.1016/S0020-7225(02)00210-0

Rao, S.S. (2007), *Vibration of Continuous Systems*, Wiley, New York, U.S.A.

Syahmazgi, M.G., Falamaki, C. and Lotfi, A.S. (2014), "A novel method for the synthesis of nano-magnetite particles", *Adv. Nano Res.*, **2**(2), 89. https://doi.org/10.12989/anr.2014.2.2.089.

Yueguang, W., Xuezheng, W., Manhong, Z., Che-Min, C. and Yilong, B. (2003), "Size effect and geometrical effect of solids in micro-indentation test", *Acta Mechanica Sinica*, **19**(1), 59-70. https://doi.org/10.1007/bf02487454

CC